Journal of Applied Polymer Science

Multiple Conjugate Electrospinning Method for the Preparation of Continuous Polyacrylonitrile Nanofiber Yarn

Jianxin He,[1,2] Kun Qi,[1] Yuman Zhou,[1] Shizhong Cui[1,2]

[1]College of Textiles, Zhongyuan University of Technology, Zhengzhou 450007, People's Republic of China

[2]Henan Key Laboratory of Functional Textile Materials, Zhongyuan University of Technology, Zhengzhou 450007, People's Republic of China

Correspondence to: J. He (E-mail: hejianxin771117@163.com)

ABSTRACT: Continuous polyacrylonitrile nanofiber yarns were fabricated by the homemade multiple conjugate electrospinning apparatus, and the principle of yarn spinning was studied. The effects of the applied voltage, flow rate, spinning distance, and funnel rotary speed on the diameter and mechanical properties of nanofiber yarn were analyzed. The diameter of the nanofibers decreased with increasing applied voltage and the flow rate ratio of the positive and negative needles (F_P/F_N), whereas the diameter of nanofibers increased with increasing overall flow rate and needle distance between the positive and negative. Subsequently, the diameter of the yarns increased first and then decreased with increasing applied voltage, F_P/F_N, and needle distance. However, the diameters of the yarns increased dramatically and then remained stable with increasing overall flow rate. The nanofibers were stably aggregated and continuously bundled and then uniformly twisted into nanofiber yarns at an applied voltage of 20 kV, an overall flow rate of 6.4 mL/h, a needle distance of 18.5 cm, and an F_P/F_N value of 5:3. With increasing funnel rotary speed, the diameters of the nanofibers and yarns decreased, whereas the twist angle of the nanofiber yarns gradually enlarged. Meanwhile, an increase in the twist angle brought about an improvement in the yarn mechanical properties. Nanofiber yarns that prepared showed diameters between 70 and 216 μm. Nanofiber yarns with a twist angle of 65° showed a tensile strength of 50.71 MPa and an elongation of 43.56% at break, respectively. © 2013 Wiley Periodicals, Inc. J. Appl. Polym. Sci. **2014**, *131*, 40137.

KEYWORDS: electrospinning; mechanical properties; nanostructured polymers

Received 19 June 2013; accepted 27 October 2013

DOI: 10.1002/app.40137

INTRODUCTION

Electrospinning is an attractive, versatile, applicable, and high-potential technique for fabricating continuous one-dimensional nanofibers.[1] Generally, electrospun nanofibers with a superfine scale, large specific surface, and porosity have potential applications in protective clothing,[2] biomaterials,[3] tissue scaffolds,[4] composites,[5] and filter and sensor materials.[6,7] However, most electrospun fibers are produced in the form of randomly oriented nonwoven fiber mats because of the bending instability of the highly charged jet.[8] The fiber mats show low mechanical properties and are randomly oriented, so the difficulty of tailoring their fibrous structure have restricted their applications.[9,10] Hence, there has been considerable interest in the development of continuous yarns made out of electrospinning nanofibers, which provide an attractive way to incorporate polymeric nanofibers into traditional textiles with a broader market.[11,12]

Recently, some researchers have reported the preparation of electrospinning nanofiber yarns. However, only a small number of researchers have obtained continuous nanofiber yarns successfully. Teo and coworkers[13,14] proposed electrospun wet spinning to prepare continuous nanofiber yarns; however, their nanofibers exhibited bad orientation and arrangement in the yarn, and for some polymers, the liquid media was hard to choose. Dabirian and coworkers[15,16] and Ali et al.[17] produced continuous yarns with two oppositely charged nozzles placed on either side of a metal disc collector, and the nanofiber bundles were aggregated and twisted by a rotating unearthed collector. Yan et al.[18] used a pair of rotating metal tubes to collect the aligned electrospun nanofibers and then twist them into yarns; meanwhile, a rotating plastic tube was inserted to wind the yarns between the metal tubes. Because the residual charges of deposit fibers in the metal tube repulse fibers that form, the nanofibers were only to be deposited partly and were arranged irregularly in the large-fiber production.

In this study, a modified multiple-needle electrospinning method, referred to as *multiple conjugate electrospinning,* was

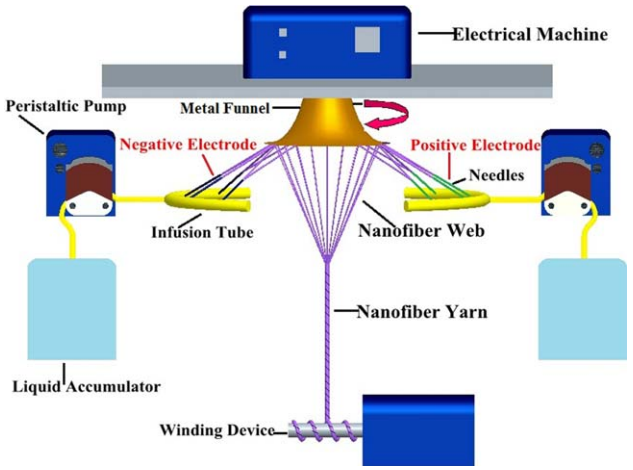

Figure 1. Schematic diagram of the multiple conjugate electrospinning apparatus. [Color figure can be viewed in the online issue, which is available at wileyonlinelibrary.com.]

applied to produce continuously twisted polyacrylonitrile (PAN) nanofiber yarns with good fiber orientation.

EXPERIMENTAL

Multiple Conjugate Electrospinning

A schematic diagram of the multiple conjugate electrospinning apparatus is shown in Figure 1. A couple of infusion tubes equipped with four needles (*i.d.* = 0.5 mm), which was connected separately to the positive and negative polarities of the high-voltage direct-current power supply, were arranged symmetrically on either side of the unearthed funnel. The take-up system was set under the funnel.

PAN (weight-average molecular weight = 70,000, Hangzhou Bay Acrylic Fiber Co., Ltd., China) was dissolved in *N,N*-dimethylformamide (Chemical Reagents Co., Ltd., China) to prepare the uniform solution with a concentration of 15 wt %. The PAN solution was transported to the needles simultaneously with uniform rates through infusion tubes by a fluid supply apparatus. Nanofibers electrospun from the oppositely charged needles deposited on the rotary funnel to form a nanofiber web that covered the funnel end. By the drawing of an insulating rod, the nanofiber web was pulled into fiber bundles. Then, the fiber bundles was twisted by a rotary funnel and wound continually to the yarn winder (diameter = 25 mm). A voltage of 14–24 kV was applied to the needles with a distance from the tip of the needle to the side of the funnel mouth of 7 cm. The distance between the positive and negative needles was 18 cm. To prevent rejection between the fibers, the distance between two adjacent needles with the same electrode could not be less than 5.5 cm. The overall flow rate of the spinning solution was varied from 5.2 to 7.6 mL/h. The take-up speed of the yarn winder was 2.0 m/min. The revolution per minutes of funnel was adjusted in the range 0–400 rpm.

Characterization

The nanofiber yarns collected were coated with gold film to observe the yarn morphologies. The instrument was a JEOL JSM-5600LV electron microscopic with an accelerating voltage of 15 kV. The average fiber and yarn diameters and twist angles were calculated on the basis of scanning electron microscopy (SEM) images. The tensile properties were measured with an INSTRON 5582 tester at room temperature (20°) under room humidity 65%. The gauge length was set to be 15 cm, and the crosshead speed was 10 mm/min.

RESULTS AND DISCUSSION

Principle and Process of Nanofiber Yarn Spinning

Figure 2(a) shows the electric field simulation of multiple conjugate electrospinning, in which two pairs of needles were positively and negatively charged, respectively, and the funnel was not earthed. After a high voltage was applied, the electric field came into being between the positive and negative needles; however, the metal funnel located in the middle of two groups of needles changed the original distribution of electric field. Electrostatic induction made both edges of the funnel have charges that were opposite to those of the nearby charged needles; thereby, there were induction fields between either edge of the funnel and their nearby charged needles. The charged jets ejected from two pairs of oppositely charged needles were attracted toward the side of the inductive funnel with opposite charges, and then, the jets were neutralized and formed a hollow nanofiber web with its edges connecting to the funnel end, as shown in Figure 2(b). After being drawn by an insulating rod placed near the central area of the funnel, the hollow nanofiber

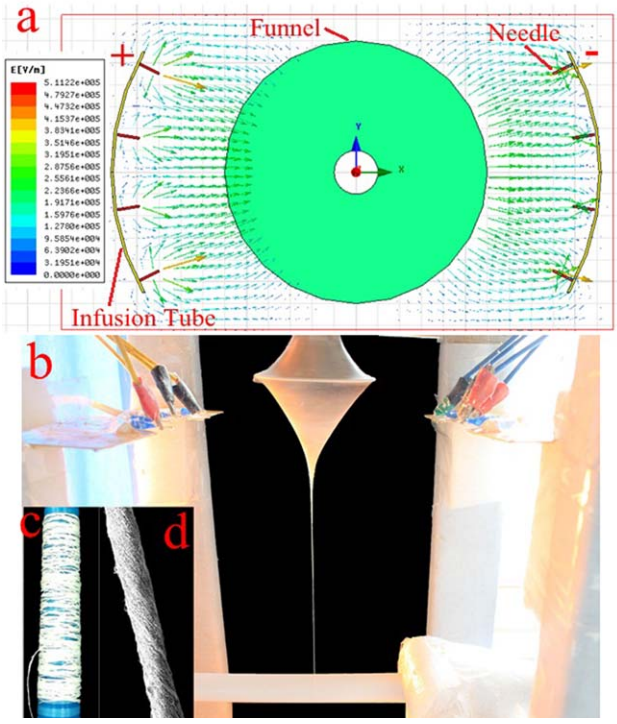

Figure 2. (a) Electric field simulation of multiple conjugate electrospinning, (b) digital camera image of nanofiber yarn spinning with the multiple conjugate electrospinning apparatus, (c) digital camera image of electrospun PAN nanofiber yarn, and (d) SEM image of a PAN nanofiber yarn. [Color figure can be viewed in the online issue, which is available at wileyonlinelibrary.com.]

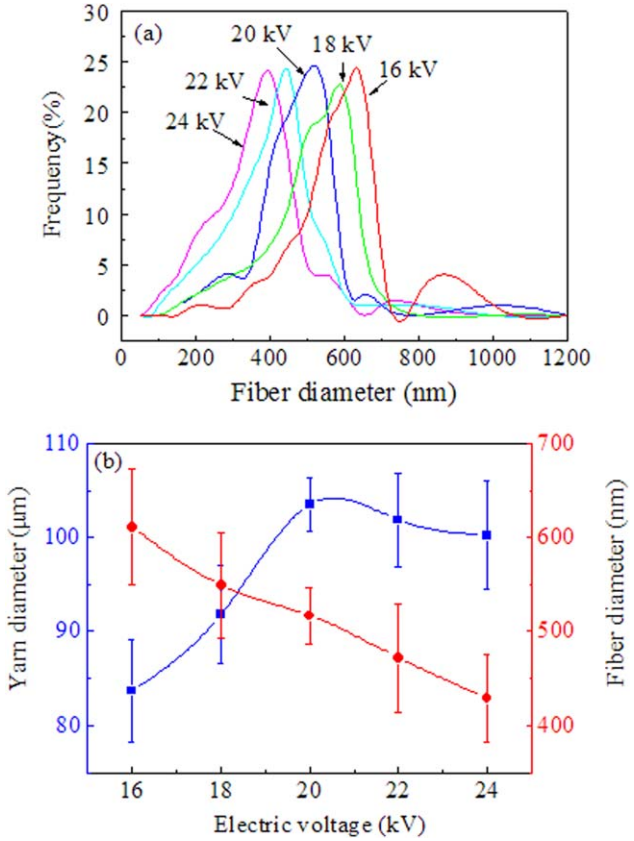

Figure 3. (a) Diameter distribution of nanofibers in yarns obtained at different applied voltages and (b) dependence of the nanofiber and yarn diameters on the applied voltage. [Color figure can be viewed in the online issue, which is available at wileyonlinelibrary.com.]

web formed a fibrous cone, with its apex attaching to the rod. Further drawing of the cone apex induced the formation of an oriented fiber bundle, which was twisted by a rotating funnel and wound onto the winder as continuous yarns. The appearance of the electrospun nanofiber yarn is shown in Figure 2(c). Figure 2(d) shows the SEM image of a twisted nanofiber yarn. In this case, once the fibrous cone was created, the subsequent electrospun nanofibers could actually deposit between the fibrous cone and the funnel. The use of oppositely charged nanofibers facilitated the formation of a stable nanofiber cone because of electrostatic attractions.

Effect of the Applied Voltage and Flow Rate on the Nanofiber and Yarn Diameters

The electric field provided the driving force for this multiple-conjugate electrospinning system. The intensity of the electric field affected not only the yarn electrospinning process but also the fiber and yarn diameters. When the applied voltage was lower than 16 kV, no yarn was formed, and only a small amount of nanofibers deposited on the funnel, apparently because of the insufficient numbers of nanofibers produced. However, when the applied voltage was above 24 kV, nanofibers were easily flowed into the air and were difficult to deposit onto the funnel. Figure 3 shows the manner of nanofiber and yarn diameters variation for various applied voltages. A higher applied voltage led to a decrease in the nanofiber diameters, whereas the diameters of the yarns increased first and then decreased as a result of the applied voltage enhancement. In the range of the applied electric voltage, increasing the intensity of electric field enhanced the drafting force and resulted in a decrease in the nanofiber diameters. When the applied voltage was lower, only a part of the solution was evolved into the Taylor cone and stretched into nanofibers. The dropping of the other of the solution led to a decrease in the total amount of nanofibers bundled. Therefore, the average diameter of the nanofiber yarns was smaller. When the voltage increased up to 20 kV, the nanofiber yarn diameters exhibited a maximal value. The reduction of the yarn diameters when the voltage exceeded 20 kV could be explained by the reduction in nanofiber deposition on the funnel under such a high voltage, which could have been derived from the unbalanced charges between the nanofibers generated from the two pairs of needles and associated charge accumulation on the funnel.

It has been established that the ratio of the flow rates between the positively and negatively charged needles (F_P/F_N) is an important parameter influencing the yarn spinning process. The dependences of the ratio of the flow rates between the positively and negatively charged needles (F_P/F_N) on the nanofiber and yarn diameters are shown in Figure 4. When the overall flow

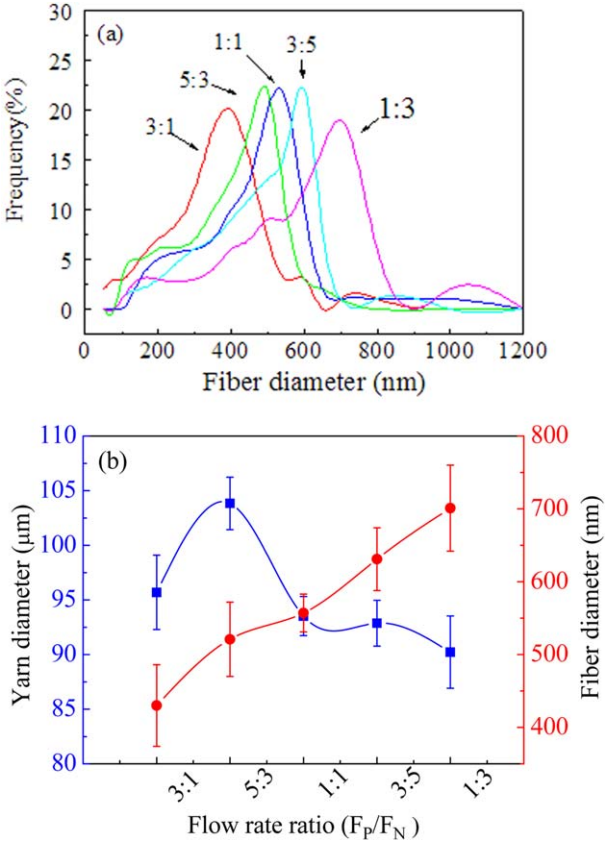

Figure 4. (a) Diameter distribution of the nanofibers in the yarns obtained with different F_P/F_N ratios and (b) dependence of the nanofiber and yarn diameters on the F_P/F_N ratio. [Color figure can be viewed in the online issue, which is available at wileyonlinelibrary.com.]

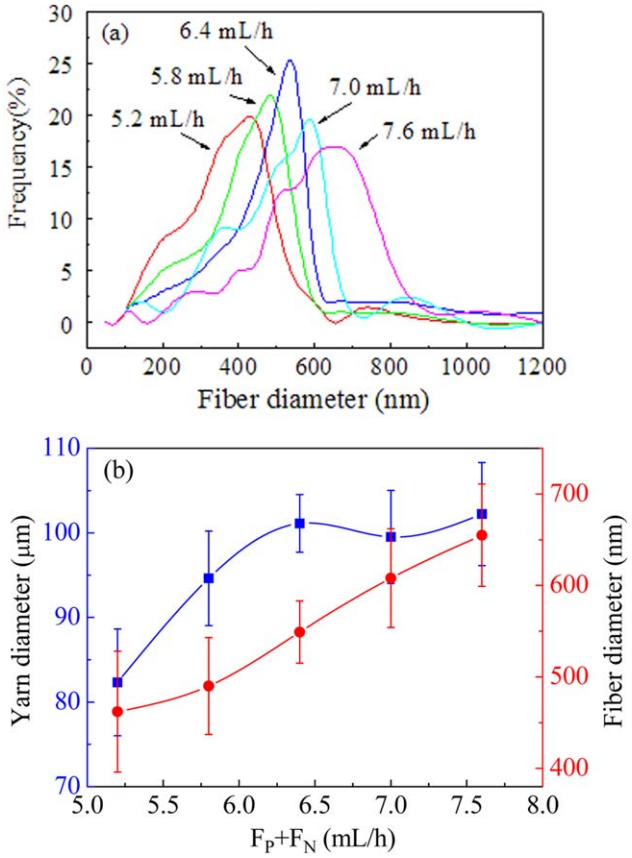

Figure 5. (a) Diameter distribution of nanofibers in the yarns obtained with different overall solution flows (F_P+F_N) and (b) dependence of the nanofiber and yarn diameters on the overall solution flow. [Color figure can be viewed in the online issue, which is available at wileyonlinelibrary.com.]

rate remained the same, the nanofibers had thinner diameters with a uniform distribution when the flow rate of positive needles was higher than that of the negative needles; otherwise, the yarn contained more thick fibers with beads. With a decrease in F_P/F_N, the nanofiber diameters increased. As shown in the electric field simulated result [Figure 2(a)], the electric field intensity of the positively charged electrospinning process was obviously stronger than that of the negatively charged electrospinning process.[19] Therefore, the positively charged needles with a higher flow rate was more conducive to the drawing of more nanofibers with uniform fineness. Otherwise, a lot of solution dropped from the needles rather than being drawn into nanofibers as the negatively charged needles had a higher flow rate. In addition, the stretched nanofibers with large average diameters could be attributed to the lower electric field intensity. Hence, the average diameter of the yarns decreased with decreasing F_P/F_N because of the decreasing of the total number of nanofibers twisted in the yarn. The nanofiber yarns showed a smaller average diameter when F_P/F_N was 3/1 because the excessive solution dropped from the needles rather than being drawn into nanofibers. Hence, nanofiber yarn spinning remained stable with a higher flow rate from the positively charged needles. Nanofiber production was supplied sufficiently, and the fiber web was formed best when F_P/F_N was 5/3.

Figure 5 shows the influence of the overall flow rate ($F_+ + F_-$) on the nanofiber and yarn diameters. When F_P/F_N was 5/3, the nanofiber diameters increased with increasing overall flow rate. However, the yarn diameters increased first and then remained stable when the overall flow rate exceeded 6.4 mL/h. When the electric field intensity remained constant and the electric force was high enough to stretch the jets, an increase in the overall flow rate resulted in an increase in the average nanofiber diameter. Meanwhile, the nanofiber yarn diameter also increased. However, the excessive solution dropped from needles rather than forming nanofibers when the overall flow rate exceeded 6.4 mL/h. In addition, disordered nanofibers were found in these yarns.

Effect of the Needle Space between the Positive and Negative on the Nanofiber and Yarn Diameters

The needle space between the positive and negative was found to influence the intensity of the electric field and then influenced the nanofiber and yarn diameters. Figure 6 shows the dependence of the nanofiber and yarn diameters on the needle space between the positive and negative. When the applied voltage remained constant, reducing the needle space between the positive and negative led to an increase in the electric field strength. Therefore, with increasing needle space between the positive and negative, the nanofiber diameters increased, and the yarn diameters increased initially and exhibited a maximal value at a space of 18.5 cm. Under a stronger electric field, the rejection among jets

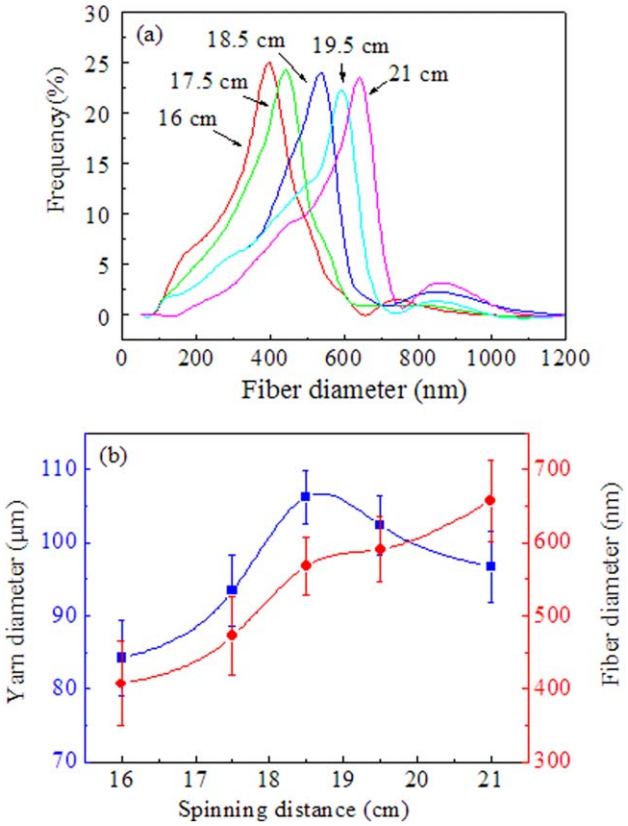

Figure 6. (a) Diameter distribution of the nanofibers in yarns obtained with different spinning distances and (b) dependence of the nanofiber and yarn diameters on the spinning distance. [Color figure can be viewed in the online issue, which is available at wileyonlinelibrary.com.]

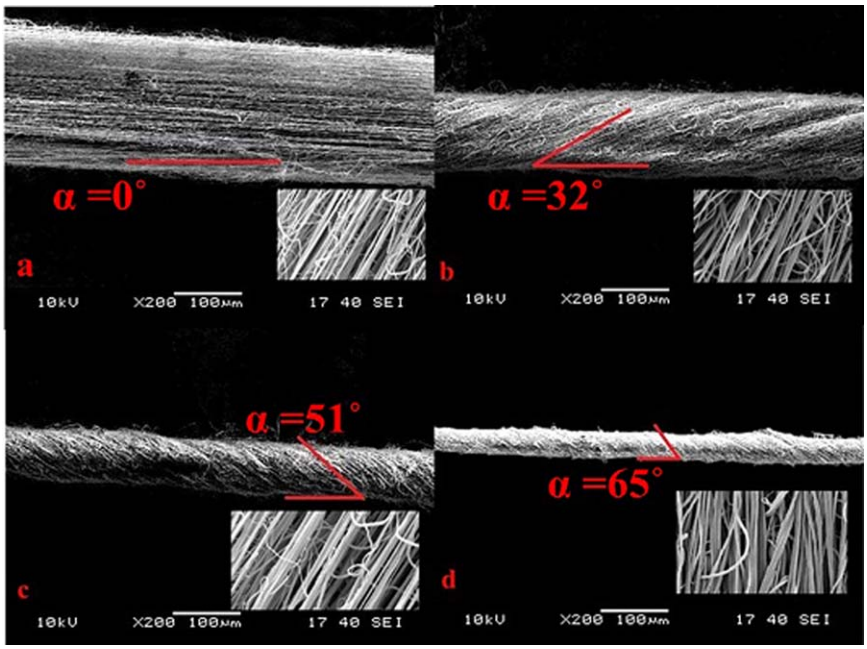

Figure 7. SEM images of the PAN nanofiber yarns with different twist angles (αs). [Color figure can be viewed in the online issue, which is available at wileyonlinelibrary.com.]

with the same charges decreased the total number of nanofibers bundled, and the adhesion among the incomplete volatile fibers limited the slipping of fibers and thus resulted in the instability of the hollow-fiber web. Moreover, the fibers were easily conglutinated on the funnel and attracted the negative electrode; consequently, they were hard to draw into a uniform continuous yarn under the needle space between the positive and negative that was less than 18.5 cm. When the nozzle space between the positive and negative was greater than 18.5 cm, with a further increase in the space, the yarn diameter decreased because of the decreased fiber deposition rate under a weak electric field. Furthermore, the space between homopolar needles could not be less than 5.5 cm to prevent the rejection among fibers. The nanofiber yarn could be stably electrospun when the needle space between the positive and negative was set at 18.5 cm and the space between the homopolar needles was 5.5 cm.

Twisted Nanofiber Yarns and Their Mechanical Properties

The SEM images were used to investigate the effect of the funnel rotation on the nanofiber morphology and yarn structure. The SEM images of the nanofiber yarns obtained at funnel rotary speeds of 0, 200, 300, and 400 are shown in Figure 7(a–d). Continuous paralleled nanofiber bundles were obtained when the funnel remained still, and the twist angle of the nanofiber yarns increased with increasing funnel rotary speed. A uniform twist distribution was observed on the surfaces of the yarns with different twist levels. The nanofiber yarn obtained at a funnel rotary speed of 400 showed a larger twist angle of 65°.

With increasing twist angle, both the tensile strength and elongation at break increased. As shown in Figure 8, the untwisted nanofiber bundles only showed a tensile strength of 2.12 MPa

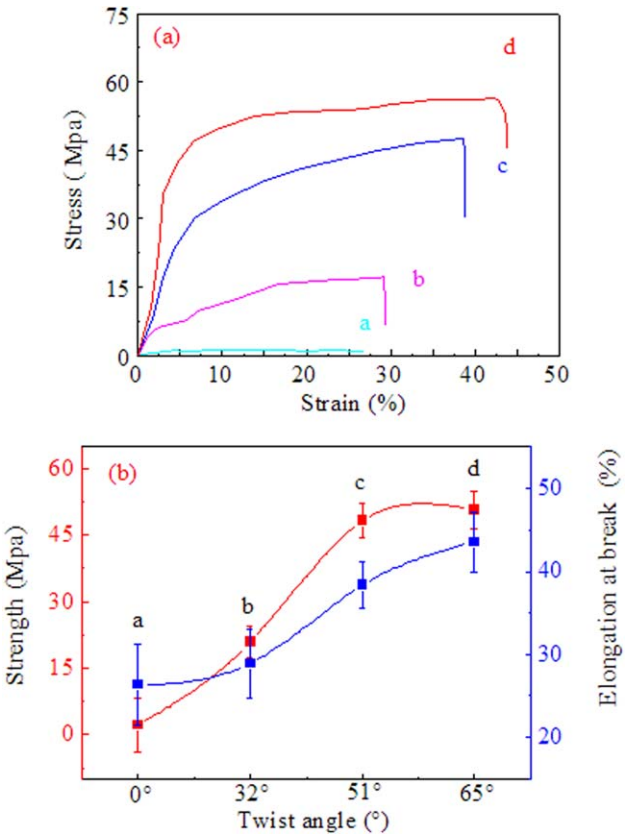

Figure 8. (a) Dependence of the tensile strength and elongation at break of the nanofiber yarns on the twist angles and (b) stress–strain curves for PAN nanofiber yarns with different twist angles. [Color figure can be viewed in the online issue, which is available at wileyonlinelibrary.com.]

and an elongation of 26.34% at break; however, nanofiber yarns with a twist angle of 65° showed a larger tensile strength of 50.71 MPa and an elongation of 43.56% at break because of the larger cohesive force between the nanofibers.

CONCLUSIONS

A homemade multiple conjugate electrospinning apparatus was used to prepare continuously twisted PAN nanofiber yarns. Electrospun nanofibers could be aggregated stably, bundled continuously, and then uniformly twisted into nanofiber yarns based on the electrostatic attraction between the nanofibers with opposite charges. Electrospun nanofiber yarns were prepared continuously and stably at an applied voltage of 20 kV, an overall flow rate of 6.4 mL/h, and an F_P/F_N value of 5:3. The twist angle of nanofiber yarns increased with increasing funnel rotary speed and take-up rate. The nanofiber yarns exhibited a tensile strength of 50.71 MPa and an elongation of 43.56% at break at a twist angle of 65°. With this method, the production of nanofiber yarns was improved when the pairs of needles were increased further. This method was also applied to prepare nanofiber yarns with multiple components.

ACKNOWLEDGMENTS

This work was supported by the National Natural Science Foundation of China (contract grant number 51203196), and the financial support of the United Foundation of the National Natural Science Foundation of China and the People's Government of Henan Province for Cultivating Talents (contract grant number U1204510) is gratefully acknowledged.

REFERENCES

1. Greiner, A.; Wendorff, J. H. *Angew. Chem. Int. Ed.* **2007**, *46*, 5670.
2. Gorji, M.; Jeddi, A. A. A.; Gharehaghaji, A. A. *J. Appl. Polym. Sci.* **2012**, *125*, 4135.
3. Kenawy, E.; Mansfield, K.; Bowlin, G. L.; Simpson, D. G. *J Controlled Release* **2002**, *81*, 57.
4. Huang, Z. M.; Zhang, Y. Z.; Kotakli, M. *Compos. Sci. Technol.* **2003**, *63*, 2223.
5. Li, D.; Xia, Y. *Nano Lett.* **2004**, *4*, 933.
6. Tsaia, P. P.; Gibson, S. H.; Gibson, P. *J. Electrostatics* **2002**, *54*, 333.
7. Lee, S. H.; Ku, B. C.; Wang, X. Mater. Res. Soc. Symp. Proc. **2002**, *708*, 403.
8. Sun, F.; Yao, C.; Song, T.; Li, X. *J. Text. Inst.* **2011**, *102*, 633.
9. Shin, Y. M.; Hohman, M. M.; Brenner, M. P.; Rutledge, G. C. *Polymer* **2001**, *42*, 09955.
10. Afifi, A. M.; Nakano, S.; Yamane, H.; Kimura, Y. *Macromol. Mater. Eng.* **2010**, *295*, 660.
11. Moon, S. C.; Richard, J. F. *Polym. Eng. Sci.* **2007**, *47*, 1530.
12. Zhou, F. L.; Gong, R. H.; Porat, I. *Polym. Int.* **2009**, *58*, 331.
13. Teo, W. E.; Gopal, R.; Ramaseshan, R.; Fujihara, K.; Ramakrishna, S. *Polymer* **2007**, *48*, 3400.
14. Yousefzadeh, M.; Latifi, M.; Teo, W. E. *Polym. Eng. Sci.* **2011**, *51*, 323.
15. Dabirian, F.; Hosseini, Y.; Ravandi, S. A. H. *J. Text. Inst.* **2007**, *98*, 237.
16. Dabirian, F.; Hosseini, S. A. *Fibers Text. East. Eur.* **2009**, *74*, 45.
17. Ali, U.; Zhou, Y. Q.; Wang, X.; Lin, T. *J. Text. Inst.* **2012**, *103*, 80.
18. Yan, H.; Liu, L. Q.; Zhang, Z. *Mater. Lett.* **2011**, *65*, 2419.
19. Kilic, A.; Oruc, F.; Demir, A. *Text. Res. J.* **2008**, *78*, 532.